On numerical modelling of sediment dynamics in the East-Frisian Wadden Sea

G. Brink-Spalink, E. V. Stanev, J.-O. Wolff

Institute for Chemistry and Biology of the Marine Environment (ICBM), Carl-von-Ossietzky-Straße 9-11, 26129 Oldenburg, Germany, email: gerold.brink-spalink@gmx.de

Abstract

Sediment transport in the East -Frisian Wadden Sea is modelled using the three dimensional, hydrodynamic k -epsilon model GETM coupled with a sediment transport model. The implemented sediment related processes include advection, vertic al mixing, settling, deposition and erosion of sediment. The mod el is run using different grain sizes which are classified in two groups: non -cohesive sediments with grain diameters larger than 63 mm and cohesive sediments with grain sizes smaller than 63 mm, the latter having the property of forming aggregates resulting in higher settling velocities. The distribu tion of sediment types show patterns comparable to the ones found in observations. The inner-tidal sediment dynamic is to a high degree asymmetric, mainly resulting from the ebb dominant hydrodynamic setting. The sensitivity of sediment transport proce sses on different wind forcing has been investigated.

Model description

The sediment transport routine is based on the equation:

$$\frac{\partial c}{\partial t} + u\frac{\partial c}{\partial x} + v\frac{\partial c}{\partial y} + w\frac{\partial c}{\partial z} = \frac{\partial}{\partial z}\left(\nu_z \frac{\partial c}{\partial z}\right) + \frac{\partial}{\partial z}(v_s c) + D - E$$

Here u, v and w are the tree velocity components, c is the suspended sediment concentration, A_ν is the vertical eddy viscosity coefficient, v_s is the settling velocity, D and E are the deposition rate and erosion rate, respectively. The settling velocity of sand is determined by Stokes formula:

$$v_s = \frac{g}{18\mu}\frac{\rho - \rho_0}{\rho_0} d^2$$

Where d is the grain diameter. The settling velocity of mud particles depends on their concentration. Higher concentrations result in a formation of larger aggregates which in turn have a larger settling velocity. This may be parameterised by:

$$v_s = k_s c^{m_s}$$

The deposition rate, D, given by Krone (1962) is:

$$D = c_b \times v_s \times \left(1 - \frac{\tau_0}{\tau_d}\right)$$

Where c_b is the suspended sediment concentration near the bottom, τ_b is the shear stress at the bottom and τ_d is the critical shear stress for deposition. The erosion rate is computed using the formula of Partheniades (1984):

$$E = M_e \times \left(\frac{\tau_0}{\tau_e} - 1\right)$$

The critical shear stress for erosion of sand is computed from Bagnold (1966):

$$\tau_e = 0.64 \rho v_s^2$$

Where ρ is the density of water and v_s is the settling velocity. The critical shear stress for erosion of mud is set constant to 0.2 Nm^{-2}. The critical shear stress for deposition is chosen to be equal to that for erosion.

The model is run using the bathymetry given in Fig. 1. A synthetic spring tide signal (Fig. 2) is used as the forcing on the northern boundary.

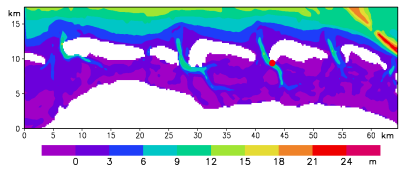

Fig. 1: Bathymetry of the East Frisian Wadden Sea in meters below mean sea level.

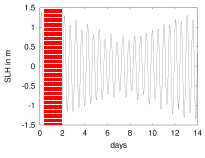

Fig. 2: Forcing tide signal at northern boundary. Red background corresponds to time shown in figures 4 and 5.

The sediment source on the bottom as a first order approximation taken to be inexhaustible for sand and mud everywhere. Effects of erosion or deposition on the bathymetry are not taken into account.

Results

In a first model run without wind forcing areas with different net transport behaviour have been determined. The resulting map can be seen in Fig. 3. The colours indicate the type of sediment most probable to be found under the conditions applied.

Time versus depth diagrams for mud and sand over three tidal cycles around spring tide at a position in the Otzumer Balje (star in Fig. 1) are shown in Fig. 4. Sand is transported near the bottom with maximum concentrations when current velocities are highest. It vanishes from the water column during slack water, whereas large amounts of the mud stay in suspension.

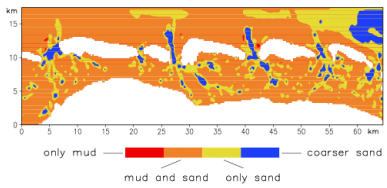

Fig. 3: Resulting map of sediment types for the no -wind scenario. Here sand has a grain diameter of 100 µm.

The maxima of mud concentrations are shifted with respect to the maxima of sand in suspension indicating that mud is still eroded and accumulates in the water column while sand already settles down and is being redeposited. The highest mud concentrations are reached approximately one hour after the highest current velocities.

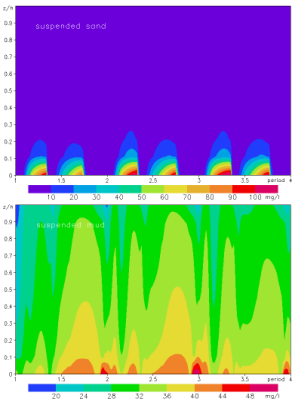

Fig. 4: Time versus depth diagrams for sand in suspension (top) and mud in suspension (bottom) at the position in the Otzumer Balje around spring tide.

The response of the sediment dynamics in the tidal basin of Spiekeroog to different wind strengths is presented in Fig. 5. In these model runs the tidal prism is equal for all wind strengths, since in all cases the same forcing tide at the northern boundary has been applied.

The vertical mean of the concentration of mud and sand in suspension can be seen in the left graphs of Fig. 5 repeating the results already seen in Fig. 4 for the no -wind case. A weak wind of 3 Bft has scarcely any effect on the sediment transport. But for 6 and 9 Bft the concentrations of mud and sand in suspension rise by a factor of approximately 1.3 and 2.5, respectively.

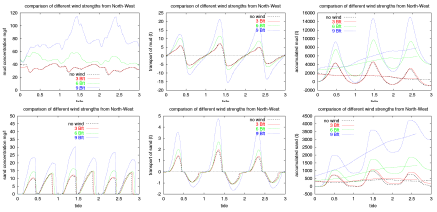

Fig. 5: Sediment dynamic for different wind -conditions (no -wind, 3, 6, and 9 Bft from north-west). First row shows mud and second row shows sand dynamics over 3 tidal cycles. Left: concentration, middle: transport through Otzumer Balje (positive for import into basin), right: accumulated sediment in backbarrier basin.

Expressed in transport through the Otzumer Balje (middle graphs) this results in a much higher transport of material during strong wind events with higher transport rates during flood. Also the tidal asymmetry described in more detail in Stanev *et al* . (2003b) can be well seen here for mud dynamics.

Clearly the different transport rates during flood and ebb must result in a net import of material into the tidal basin for wind y conditions. This is illustrated in the right graphs of Fig. 4, where the accumulated sediment is plotted. Also the mean over one tidal cycle is plotted to filter out the tidal signal. Whereas for no -wind and low -wind (3 Bft) conditions no net sand transport occurs and mud is even exported from the inlet, both mud and sand are being accumulated when strong winds are active from north-west.

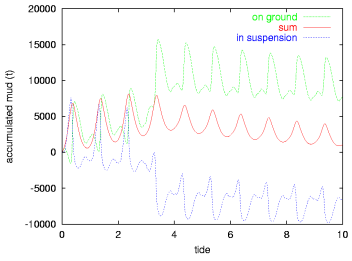

Fig. 5: Accumulated mud in the tidal basin of Spiekeroog with wind from north -west (6 Bft) for three tides. At the beginning of the fourth tide the wind was switched off. The topmost curve is the mud accumulated on the ground of the basin, the bottom curve is mud in suspension inside the basin, and the middle curve is the sum of both. The accumulated mud was set to zero at the beginning of the first tide.

This import of mud during strong wind events was also measured by Santamarina & Flemming (2000) for the same tidal inlet. To determine the fate of the material after a stron g-wind event, the wind has been switched off after some tidal cycles. The results are shown in Fig. 5. In the moment of turning off the wind a large amount of the mud in suspension settles down increasing the accumulated mud on the ground of the basin. During the following tides the mud is gradually exported through the inlet as could be assumed from Fig. 4 (top right).

In all these runs wind induced surface waves have not been considered, which could dramatically effect the erosion of sediment in shallow waters. This might counteract the import of sediment during storm and will be a topic of future work.

Conclusions

The presented hydrodynamic model GETM together with the sediment transport model is a successful tool to theoretically investigate the sediment transport behaviour of the East Frisian Wadden Sea. Comparisons with measurements have shown the high accuracy of the hydrodynamic model. It is also capable of simulating the observed tidal asymmetries which have an important influence on the transport of the suspended sediment load.

Although the hydrodynamic model has been tested many times in the last years and can be considered well calibrated, the sediment transport model has still to be adjusted by comparison with measurements. A more detailed analysis of the interaction of the tidal asymmetry and the sediment transport will be a topic of future work.

References

Arakawa, A.& Lamb, V. R. (1977) Computational design of the basic dynamical processes of the UCLA general circulation model. Meth. Computat. Phys, **16**, 173-263.

Bagnold, R. A. (1966) An approach to the sediment transport problem from general physics. USGS Prof. Paper, **4421**, 37 pp.

Burchard, H. & Bolding, K. (2002) GETM - a general estuarine transport model. Scientific documentation. No EUR 20253 EN, European Commission, printed in Italy, 157 pp.

Krone, R. B. (1962) Flume studies of the transport of sediment in estuarial shoaling processes. Final Report, Hydraul. Eng. Lab., Sanitary Eng. Res. Lab., Univ. of California, Berkeley, 110 pp.

van Leussen, W. (1988) Aggregation of particles, settling velocity of mud flocs, review. In: Dronkers, J. & van Leussen, W. (eds.), Physical processes in estuaries, Springer, Heidelberg, 347-404.

Mehta, A. J. (1988) Laboratory studies on cohesive sediment deposition and erosion. In: Dronkers, J. & van Leussen, W. (eds.), Physical processes in estuaries, Springer, Heidelberg, 327-345.

Partheniades, E. (1984) A fundamental framework for cohesive sediment deposits. In: Mehta, A. J. (ed.), Lecture notes on coastal and estuarine studies 14, Estuarine cohesive sediment dynamics, Springer, Heidelberg, 219250.

Puls, W. & Sündermann, J. (1990) Simulation of suspended sediment dispersion in the North Sea. In: R.T. Cheng (ed.), Coastal and estuarine studies, **38**, Residual currents and long-term transport, Springer, New York.

Rodi, W. (1980) Turbulence models and their application in hydraulics. Report Int. Assoc. for Hydraul. Res., Delft, Netherlands.

Santamarina, C. P. & Flemming, B. W. (2000) Quantifying concentration and flux of suspended particulate matter through a tidal inlet of the East Frisian Wadden Sea by acoustic doppler current profiling. In: Flemming, B. W., Delafontaine, M. T. & Liebezeit, G. (eds.), Muddy coast dynamics and resource management, Elsevier, Amsterdam, 39-51.

Stanev, E., Flöser, G. & Wolff, J. -O. (2003b) Dynamical control on water exchanges between tidal basins and the open ocean. A case study for the East Frisian Wadden Sea. Ocean Dynamics, PECS 2002 Special Issue.

Stanev, E., Wolff, J. -O., Burchard, H., Bolding, K. & Flöser, G. (2003a) On the circulation in the East Frisian Wadden Sea: Numerical modelling and data analysis Ocean Dynamics, **53**, 27-51.